Chapter 5

INVESTIGATION OF CAVITATION IN GLASS-FORMING LIQUIDS

ABSTRACT

In an effort to better understand the source of toughness in metallic glass, we have investigated cavitation in glass-forming liquids. When subjected to negative hydrostatic pressure, a liquid will reduce its energy through the formation of a cavity. This phenomenon is the competing process to shear band growth and the development of a large plastic zone, which we have identified as the crucial parameter for the wider adoption of metallic glass as an engineering material. We report the homogeneous and heterogeneous nucleation of cavities in $Zr_{41.2}Cu_{12.5}Ti_{13.8}Be_{22.5}Ni_{10}$ (Vitreloy 1) liquid by the application of a critical negative pressure. For homogeneous nucleation, we estimate a critical negative pressure of less than 500 MPa at a temperature of roughly 1000 ºC and a timescale of ~7 s. The heterogeneous nucleation of cavities is observed and is estimated to take place at much smaller negative pressures, thus an important finding as this easy pathway to cavitation represents a limiting factor for plastic zone development in metallic glass. When liquid Vitreloy 1 is subjected to a negative pressure less than the critical pressure for homogeneous nucleation on a laboratory timescale of 1 to 7 s and is free of heterogeneous nucleation sites, no cavities are formed. The liquid is thus "metastable" on laboratory timescales with respect to cavitation at these temperatures and estimated negative pressures.

INTRODUCTION

The role of shear banding has been discussed extensively in the shielding of the crack tip by the plastic zone when metallic glass is loaded in mode I fracture conditions [1,2]. This is the sole toughening mechanism in monolithic bulk metallic glass [3]. The Poisson's ratio has been recognized as an important parameter in determining the fracture toughness of a metallic glass [4] as it is a reasonable representation of a glass's ability to promote shear banding before cavitation in the shear band extends the crack further in to the material [1]. Dimpled fracture, a sign of cavitation, has been observed for amorphous metal in loaded both in tension and in bending [5,6]. The fact that a solid can fail by a phenomenon generally reserved for fluids is an important realization. The once-frozen glass inside the shear band is actually now moving in a state of plastic shear flow at an elevated temperature and potential energy [7,8]. Critically, the fluid inside the shear band is also subject to an opening tensile stress. This opening stress is the source of cavitation and crack propagation in metallic glass. Understanding this phenomenon in greater detail would shed light on a crucial aspect of toughness in metallic glass. If the negative pressure at which a cavity nucleates in the liquid could be determined as a function of the liquid temperature, one could predict where cavitation is expected to occur in an operating shear band of a deforming metallic glass. In turn, this would enable more accurate modeling of the fracture toughness of a solid metallic glass under mode I crack opening.

Cavitation cannot be avoided for any fluid that is placed in a state of triaxial tension (negative hydrodynamic pressure) as the liquid is always metastable to cavitation in this stretched state. The intermolecular forces of the fluid can keep it together for some pressure- and temperature-dependent time, but the fluid would always rather decompose in to some vapor and a less stretched fluid [9]. The chemical potential of the gas goes to negative infinity as the molar volume gets large, so the vapor phase is always favored. There is no such thing as gas at a negative pressure as at high molar volumes all gases behave as an ideal gas, which is already so sparse that it does not have the intermolecular forces to resist the pull of a negative pressure.

Molecular dynamics simulations by G. Duan in his thesis [10] established an equation of state for the $Zr_{54}Cu_{46}$ bulk glass-forming liquid. The equations of state established by G. Duan were used by An, Garrett, et al. to calculate the temperature-dependent spinodal pressure of the liquid (the pressure at which the bulk modulus vanishes and the barrier to nucleation of the vapor phase vanishes) [11]. The system was also stretched to various negative pressures and temperatures and allowed to sit for ~1 ns at each pressure and temperature. If the system cavitated within the timescale of the simulation, it was marked as the critical cavitation pressure for that temperature. In this fashion the temperature-dependent cavitation pressure was determined, which was about half the negative pressure of the spinodal pressure. While the strain and sample size are vastly different from the laboratory timescale, it is still interesting to see that the metallic liquid responds to negative pressure in a manner similar to other fluids. Our molecular dynamics work was started just before the experimental work was started, and the molecular dynamics study continued after the experimental work was discontinued. The paper by An, Garrett, et. al. [11] was actually received by its publisher one day before a molecular dynamics study of cavitation by Murali et al. [12] was received by their publisher! They also studied cavitation in binary metallic glasses, and they also find that cavitation is controlled by fluctuations in the glass that will form cavities once they reach a critical size. Their study shows how the fluctuations and their resulting cavitation behavior differ between a brittle and tough glass-forming liquid [12]. It is an interesting study that is motivated by the same curiosity about the origins of toughness in metallic glass as this work. For this chapter, we set out to explore cavitation in bulk glass-forming liquids by placing them in a pure state of negative hydrodynamic pressure (all cross terms in the stress tensor are zero and the trace of the stress tensor is negative). While our primary goal is bulk glass-forming metallic liquids, we also make a brief detour through organic glass formers.

EXPERIMENTAL METHODS

In the molecular dynamics simulations mentioned above, it is trivial to apply a negative hydrostatic pressure. However, in the laboratory, it is much more difficult to apply a pure negative hydrostatic pressure without any additional shear-stress components. Uniaxial tension and bending are the two main methods that apply some opening stress on a material, but none of these methods provides a pure triaxial negative stress on the material. We specifically wanted a pure negative hydrostatic stress placed on a metallic glass-forming liquid. M. L. Lind demonstrated homogeneous cavitation in the liquid of the glass-forming organic molecule glycerol by quenching a fused silica cylinder capped with a copper plug in to a liquid nitrogen bath [13]. This experimental setup creates negative pressure in the liquid inside the container by taking advantage of the difference in the coefficient of thermal expansion between the liquid glycerol and the glassy solid glycerol. The outside of the container is cooled below the glass transition temperature T_g which cools the liquid near the edges of the container first, which results in a solid glassy container with a liquid interior. As this container cools further, the volume of the solid shell shrinks at a rate much slower than the volume of the liquid interior. This difference in volumetric shrinkage puts the solid shell in compression and the liquid interior in triaxial tension without any shear components. The cylindrical container of Lind made it difficult to estimate the pressure at which the glycerol was cavitating, we experimented with different designs of fused silica containers that might allow for better estimation of the pressure. We settled on a spherical geometry that would allow for a near uniform cooling and simple estimation of pressure, we will discuss estimation of pressure later. The final design shown in figure 5.1(a) is a near perfect sphere attached by a thin (2 mm inner diameter) neck to a standard fused silica tube. The thin neck that connected the sphere to the quartz tube is a key design feature that was not well understood at the onset of the experiments. The original design had neck diameters that were much too large and thus the liquid inside the neck did not solidify early enough to prevent reflow of the hot liquid from the upper tube through the neck and in to the sphere. Once the neck diameter was reduced sufficiently, the liquid in the neck solidified quickly in the quench process and mechanically encapsulated the sphere, allowing for proper cavitation experiments with the buildup of negative hydrostatic pressure. The Caltech glass blower custom made each fused silica tube and was integral in the design process. The diameter of the ampule could be varied, but they were always attached with a similarly thin neck to a 10 mm inner diameter and 12 mm outer diameter fused silica tube about 18 inches long. The dimensions of the neck were kept constant at an inner diameter of ~2 mm, an outer diameter of ~4 mm, and a wall thickness of 1 mm to ensure reproducible freezing in the neck.

We unwittingly reinvented a modified Bertholet tube [14]. While the original design operates on the same principle of hot liquid shrinking inside a rigid container, the Bertholet tube was sealed shut at high temperature and then cooled slowly to apply negative pressure. Our design relies on the freezing of the hot liquid inside the neck of the tube to form a solid metallic glass plug that becomes part of the rigid container that mechanically encapsulates the hot liquid center of the sphere. In contrast to the Bertholet method, we are unable to cool our design slowly as our glass-forming liquid would crystallize before cavitation could take place. If the cooling were roughly quasi-static, we could perfectly predict the volume strain and negative pressure from the thermal shrinkage. Since the quenching process is dynamic we can't determine exactly what the negative pressure on the liquid inside the sphere is, but we know that as long as there is liquid above T_g inside a solid sphere, there will be some amount negative pressure built up in the liquid. We employ different diameter ampules and vary the initial temperature T_o to induce different levels of thermal volume strain in the hot liquid. The details of estimating the volume strain and pressure will be handled in the discussion section.

The general guideline for how these cavitation experiments were conducted is as follows. Start by measuring the volume of the fused silica sphere. It is useful to graphically measure the inner and outer diameter of the sphere to estimate volume, but I found that I trusted a direct volumetric measurement much more. Using a fluid that has a low enough surface tension so that it can easily traverse the 2 mm inner diameter neck, it was easy to simply fill the sphere and measure the volume of the fluid directly with a graduated cylinder. Once the volume of the sphere is known, the appropriate mass of metallic glass can be calculated for the experiment. It is best to overfill the sphere by at least 10 to 20% so that the neck between the tube and ampule is completely filled. For both the metallic glass and the organic glass-former, we typically used two heat sources, a hot furnace for preparing the material and filling the sphere, and sometimes a cooler one for equilibrating the filled sphere at the desired temperature for quenching. A high temperature, well above the liquidus temperature, is necessary to obtain a homogeneous melt and bring the liquid to a low enough viscosity to infiltrate the neck of the sphere. The organic glass-formers must only be heated ~100 ºC above its glass transition temperature, or to the boiling point of water (to remove absorbed water that could act as heterogeneous nucleation sites), whichever temperature is higher.

Once the tube has been filled with cleaned and weighed material it can be placed in the hotter furnace. Vacuum can be applied to aid with degassing or dehydrating. When the material has stopped bubbling, the vacuum is removed and the sphere is given a moderate overpressure of 5 to 20 psi. Gently tapping the tube can help the process, but it is common to repeat the vacuum and overpressure cycle four or more times to completely fill the sphere. The full sphere is then allowed to sit under vacuum for two minutes to make sure any small bubble can rise up through the neck and our of the sphere. When complete, the sphere is brought to atmospheric pressure or slight overpressure of a few psi before it is transferred to the cooler furnace or bath (if using). After the sphere has equilibrated at the appropriate temperature, the sphere is quickly plunged in to the quench bath to cool the sphere as quickly and evenly as possible below the glass transition temperature of the glass-forming liquid inside. Information about specific intermediate temperature heat sources and quench baths will be included in the results section for each glass-former utilized. Also, during or after quenching, the negative pressure built up on the inside of the sphere is often enough large enough to exceed the compressive strength of the fused silica tube. The fused silica tube would always break gently when quenching the metallic liquids, which did not cause a safety issue, but required one tube for each experiment. The fused silica tube would sometimes survive the quenching of the molecular glass-formers, which could then be reheated and quenched again. However, when the ampules containing the molecular glass-formers did break, they would rupture violently and send glass everywhere; safety was a must.

EARLY RESULTS WITH $Pd_{43}Cu_{27}P_{20}Ni_{10}$, GLYCEROL, AND BORON OXIDE

The $Pd_{43}Cu_{27}P_{20}Ni_{10}$ alloy was the first liquid used in this work. Pd-based glass is an attractive candidate for this experiment because it is an excellent glass former with >1 cm critical casting diameter, and it does not chemically react with our fused silica container. That means it could be recycled and used for many experiments, avoiding the hassle of producing new material for each experiment. Unfortunately, $Pd_{43}Cu_{27}P_{20}Ni_{10}$ also does not wet fused silica, meaning that it prefers to stay closer to itself than the wall of the fused silica container. All cavitation experiments with this Pd-based alloy were quenched from 1000ºC and ended up with samples that closely resembled figure 5.1(b).

We found that if the liquid does not wet the quartz there is no way to evenly remove heat from the outer shell of the liquid on the top of the sphere. The direction of quenching, bottom first, results in the liquid at the bottom of the sphere cooling faster than the liquid at the top of the sphere. Since the liquid does not wet the fused silica, the liquid in the top of the sphere pulls away from the fused silica wall as the liquid in the bottom of the sphere shrinks from cooling. Once any part of the liquid has pulled away from the fused silica wall, that liquid is not in contact with the quench bath and will not vitrify in to a glass. This also prevents the sphere from being mechanically encapsulated. Instead of generating negative pressure in the sphere, the thermal volume strain is expended on growing arge cone-shaped divots that run toward the center of the sphere. These cones are liquid reflow of the last hot liquid left to cool in the sphere; they effectively absorb all the volume strain that should have been produced in the center of the sphere. Because of this we had to abandon Pd-based glasses and explore liquids that wet fused silica.

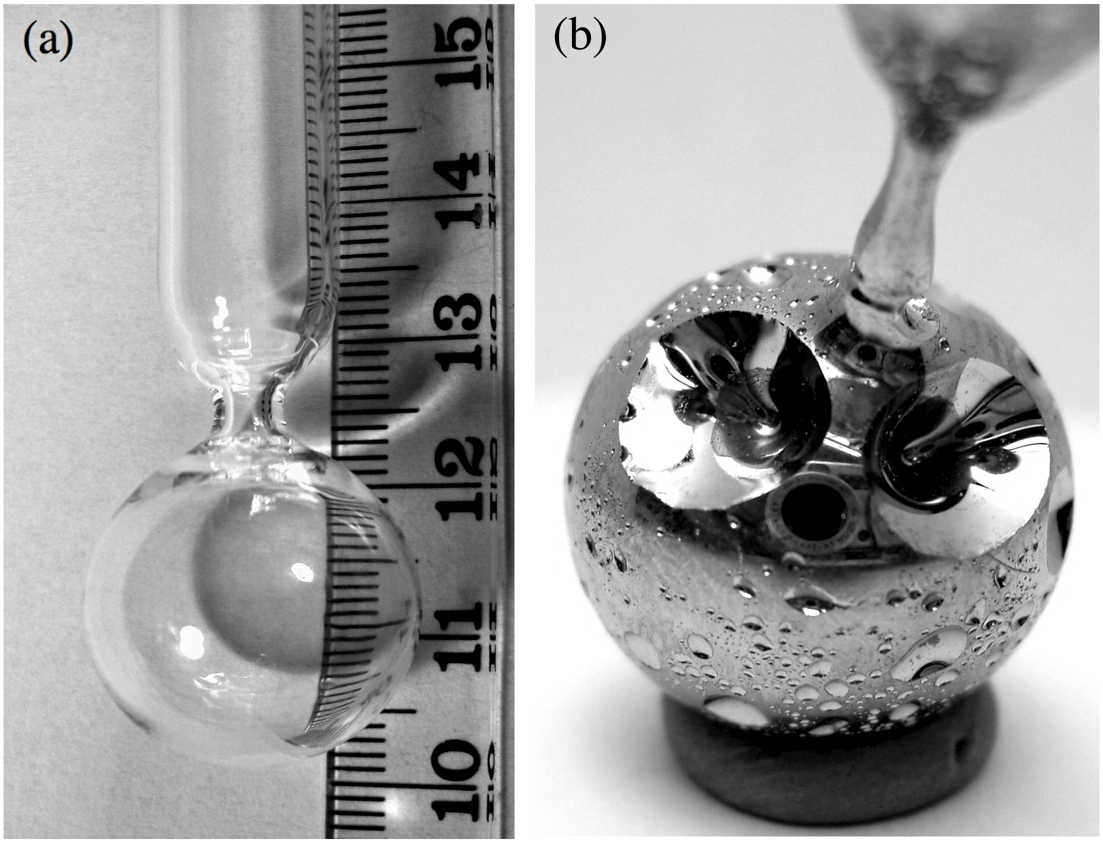

Figure 5.1 (a) The final shape design of fused silica ampule that was used for all experiments in this work. The ampule diameter can be varied but the neck and tube were kept constant. (b) A representative cavitation experiment sample of $Pd_{43}Cu_{27}P_{20}Ni_{10}$ glass displaying how all the volume strain from quenching the hot liquid is absorbed at the top surface of the sphere because the liquid does not wet the fused silica.

While the Pd-based glass did not work out as we hoped, we did experiment with different liquids for thermal transfer in the heat bath. The original quench bath for the Pd-based glass experiments was water, and we though that perhaps the boiling of water during the initial quench from 1000 ºC was preventing effective cooling of the top hemisphere. This initiated a search for an effective heat transfer liquid with a high thermal diffusivity and high boiling point. We eventually decided on a low melting point metal alloy of $Bi_{50}Pb_{26.7}Sn_{13.3}Cd_{10}$ (Wood's metal / Cerrobend) that has a eutectic melting point of 70 ºC, a large density of 9.4 g/cm^3, and a boiling point and thermal diffusivity much higher than that of water. We continued to use this alloy for all metallic glass quench baths as it provided an even and robust quenching.

Once we proved that this container design could produce a thermal volume strain but were continuously frustrated with the performance of the Pd-based glass, we thought it would be fruitful to test molecular glass-formers. Since Dr. M. L. Lind had already demonstrated cavitation in glycerol quenched in liquid nitrogen [13], we attempted to replicate her results. The T_g of glycerol is an extremely low -83 ºC (190 K), necessitating the use of liquid nitrogen as a quench bath, which boils at −196 °C (77 K). The glycerol was brought above 100 ºC for degassing and dehydrating under vacuum, from there it was quenched into a liquid nitrogen bath inside of a double-walled vacuum Dewar with a window so that the cavitation could be viewed *in-situ*. A representative picture from one of these experiments is shown in figure 5.2(a). The initial temperature for the glycerol experiments was varied from 25 ºC to 100 ºC. Every attempt with glycerol resulted in cavitation, preventing us from establishing a critical cavitation pressure. Also, the fused silica tubes did not survive more than a handful of quenches to liquid nitrogen temperatures, prompting the search for a different molecular glass former.

Boron oxide B_2O_3 was being used as a flux for the Pd-based glass, but it is also a strong glass-former that is highly resistant to crystallization. It has a moderate T_g of 263 ºC (563 K) and a melting temperature of 477 ºC (750 K). For boron oxide, the main worry was properly degassing and dehydrating the melt while simultaneously preventing the melt from blowing out of the top of the tube from the massive amounts of bubbling when vacuum was applied. The positive trade-off is that boron oxide is so resistant to crystallization that it can be cooled in air at room temperature instead of quenched in a bath. This was particularly nice as it allowed for video recording of the entire cooling process. To aid in the freezing of the neck, compressed gas was directed at the neck of the tube for an increased cooling rate. Figure 5.2(b) shows a sphere of boron oxide recovered after cavitation. Both the fused silica ampule and boron oxide sphere sample shattered during the experiment. The cavity is filled with modeling clay to better visualize the size of the cavity, which is about 16% of the sphere volume.

Both boron oxide and glycerol were never quenched in a manner where they did not cavitate, so we were unable to establish a critical cavitation pressure. Only a modest amount of time was spent experimenting with the organics, as we really wanted results for a metallic glass-former. However, it was an instructive exercise and a proof of concept for the experiment. We could watch as the cavities form in situ inside the optically transparent organic glass-formers. We confirmed that cavities can nucleate homogeneously in our experimental setup, and that they mainly nucleate in the center of the top hemisphere. This effect is likely caused by the reduced cooling rate in the top of the sphere. Another important observation is that only a single cavity nucleates in any of the spheres. Once one cavity reaches the critical size, it grows and relieves all the mechanical energy stored in the rest of the liquid. This single cavity can relieve all the negative pressure in the sphere by growing to a larger size, preventing any other cavities from forming as the rate of cavity formation is highly dependent on the negative pressure and temperature of the liquid [11].

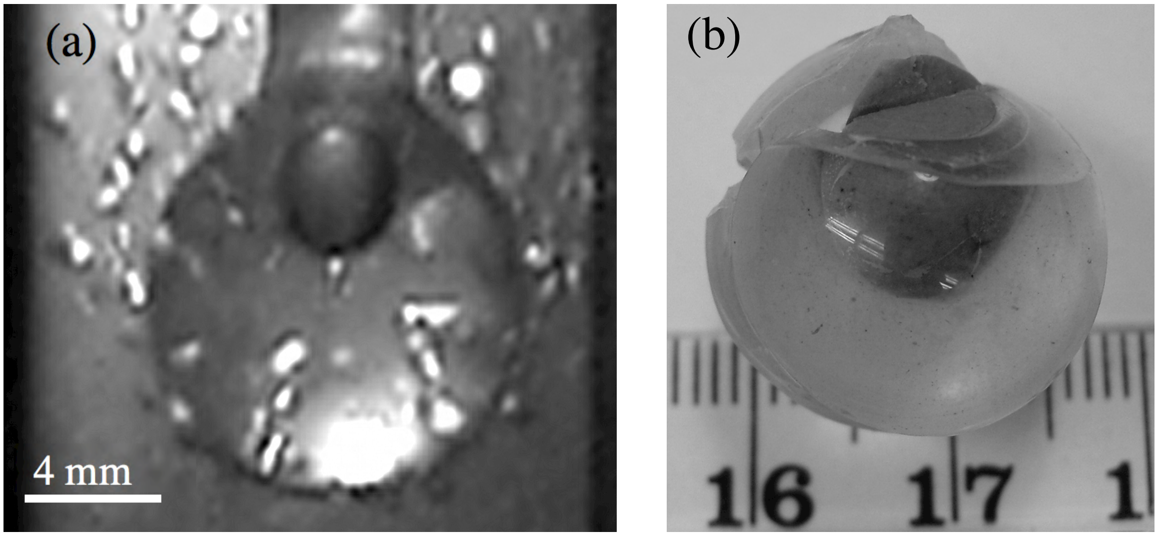

Figure 5.2 (a) An in situ picture of the molecular glass-former glycerol $C_3H_8O_3$ inside a fused silica ampule with a homogeneously nucleated cavity when quenched from room temperature 300 K into liquid nitrogen at 77 K. (b) A sphere of boron oxide B_2O_3 with a homogeneously nucleated cavity that has been filled with clay to elucidate the volume of the cavity inside the translucent boron oxide.

RESULTS AND DISCUSSION FOR $Zr_{41.2}Cu_{12.5}Ti_{13.8}Be_{22.5}Ni_{10}$

The well-studied family of Zr-based alloys relies on elements with a strong affinity for oxygen that will aggressively chemically react with a fused silica tube. This reaction creates a strong interphase layer of mixed intermetallics that act as a glue to hold the liquid to the surface of the fused silica. This allows for even heat transfer out of the shell of the sphere so that as much thermal strain as possible can be transferred to the hot liquid in the center of the sphere. The $Zr_{41.2}Cu_{12.5}Ti_{13.8}Be_{22.5}Ni_{10}$ (Vitreloy 1 or Vit1) liquid was always brought to at least an initial temperature of 1000 ºC to exceed the liquidus temperature of ~915 ºC. This high temperature was also necessary to lower the viscosity of the liquid enough to allow for complete filling of the fused silica ampule. An intermediate heat source was often used to change the temperature of the ampule before the quench. If the desired temperature was well above 580 ºC, the "nose" temperature of the time-temperature-transformation (TTT) diagram, a second furnace was sufficient to radiatively cool the sample to the new moderate temperature. However, for temperatures close to 580 ºC, it was necessary to utilize the rapid heat conduction provided by a tin bath to quickly equilibrate the ampule to the new temperature, typically 650 ºC or 700 ºC. The T_g of Vit1 is 345 ºC and was routinely quenched from 1000 ºC in to an ~80 °C quench bath of the fusible alloy Wood's metal. After quenching, the fused silica shell always spalls off the frozen Vit1 sphere by a mode II crack that propagates parallel to the quartz/glass interface, halfway through the thickness of the quartz. This left about a half millimeter of fused silica covering the glassy sphere, shown in the rough specular surface of the Vit1 sphere shown in figure 5.3. To facilitate more accurate measurements of the final sphere diameter, a dremel tool was used to mechanically remove any remaining quartz. After the density of the sphere is measured by the Archimedes technique, the sphere is sectioned with a 0.5 mm thick diamond impregnated blade. If there is a cavity, the cavity volume can be estimated with either graphical methods or by weighing the amount of clay (of a known density) it takes to fill the cavity. With both methods, one must remember to include the volume removed by the cut. If there is no cavity apparent on the cut surface, we check for other cavities in the sphere by measuring the density of both sphere halves to see if they are in agreement with each other and the original density of the entire sphere. We only witnessed cavities forming on the centerline of the top hemisphere, just like the cavities found in the molecular glass-formers.

Notice in figure 5.3 that the exterior of the sphere is particularly dark in color, especially when compared to the shiny exterior of the Pd-based glass, and is the intermetallic layer that kept the liquid wetted to the fused silica during the quenching. Unlike the molecular glass-formers, we observed heterogeneous nucleation of cavities in the Vit1 samples, such as the cross section of the sphere in figure 5.4. The heterogeneously nucleated cavity forms off the top wall of the fused silica container and then grows inward as the sphere cools. These cavities grow to a large volume of ~1% of the sphere volume. To contrast the heterogeneous formation of cavities, in figure 5.5 we present the cross sections of a sphere with a homogeneously nucleated cavity and a sphere without any cavities. Both spheres have a volume of approximately 0.75 cm^3, but were quenched from different temperatures. The sphere quenched from 1000 ºC cavitated homogeneously in the center of the sphere, and the sphere quenched from 700 ºC did not cavitate heterogeneously or homogeneously. The sphere quenched from 700 C avoided heterogeneous nucleation of cavities from the wall of the container, but did not have enough thermal volume strain to generate a negative pressure that exceeds the critical pressure for homogeneous cavitation at that temperature. Alternatively, it could be that the amount of time the negative pressure was applied was not long enough for a cavity to nucleate, as a liquid is always metastable at any negative pressure [11,15]. Now that all three types of experimental results have been presented, we will discuss the results of all the Vit1 cavitation experiments.

Figure 5.3 A representative example of $Zr_{41.2}Cu_{12.5}Ti_{13.8}Be_{22.5}Ni_{10}$ liquid after quenching in the fused silica container shown in figure 5.1(a). Fused silica remains attached to the dark-colored intermetallic on the exterior of the sphere formed by the chemical reaction between the Vit1 liquid and the fused silica container.

Figure 5.4 The cross section of the $Zr_{41.2}Cu_{12.5}Ti_{13.8}Be_{22.5}Ni_{10}$ sphere shown in figure 5.3, this sample was quenched from 650 ºC. A cavity formed during quenching but it appears to have nucleated heterogeneously at the top wall of the fused silica container near the neck of the ampule. As the interior liquid cooled, the cavity grew from the container wall toward the center of the sphere, resulting in a highly elongated cavity that is ~1% the volume of the sphere.

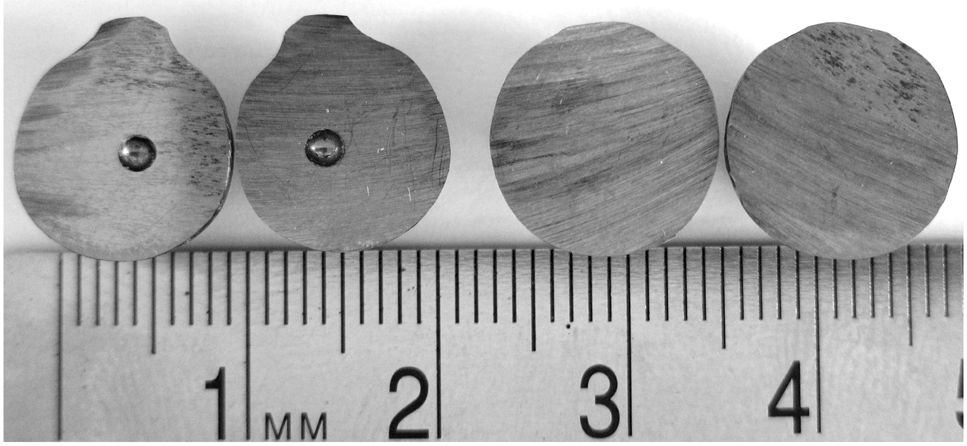

Figure 5.5 Cross-sectioned spheres of $Zr_{41.2}Cu_{12.5}Ti_{13.8}Be_{22.5}Ni_{10}$ liquid that were quenched in fused silica from different temperatures. Both spheres have a volume of ~0.75 cm^3. The sphere with the cavity was quenched from 1000 ºC, and the sphere with no cavity formation was quenched from 700 ºC. The central placement of the cavity in the sphere quenched from 1000 ºC and its uniform diameter suggest homogeneous cavitation of the liquid upon reaching a critical negative pressure on the order of seconds. The sphere quenched from 700 ºC supported some amount of negative pressure in its liquid during cooling, but the critical negative pressure for laboratory timescale homogeneous cavitation was not reached.

Table 5.1 contains the sphere volume, initial temperature T_o, ΔT (the difference between T_o and T_g, where T_g = ~345 ºC [16]), temperature-dependent bulk modulus $B(T_o)$ (estimated from the highly similar liquid $Zr_{46.75}Ti_{8.25}Cu_{7.5}Ni_{10}Be_{27.5}$ [17]), cavity nucleation type, and the cavity volume as the percentage of sphere volume for all of the Vit1 liquid cavitation experiments. We also include in table 5.1 our estimations of the maximum potential volume strain and maximum potential negative pressure. We call this the "maximum potential" because it relies on the assumption that the sphere quenches quasistatically and is fully encapsulated at the beginning of the quench (our samples require that the liquid inside the neck to the ampule solidify before negative pressure can build). This simple model also assumes that the container is infinitely rigid and would not contract in response to the negative pressure building in the center of the sphere. We note that the Young's modulus of glassy Vit1 is about 30 GPa greater than fused silica, so any solid Vit1 formed during the quench is a much stiffer container than the fused silica, reducing the overall compliance of the container. Between the delay in the freezing of the neck, the compliance of the solid shell, and the time-dependent development of negative pressure from volume contraction, the amount of negative pressure that is actually experienced by the liquid is some unknown percent of the quasistatically quenched upper bound. However, we do expect that as the sphere diameter increases, the time that it takes for the liquid inside the neck to solidify decreases as compared to the total quenching time.

The upper bound of thermal volume strain can be estimated from

$$\varepsilon_{\max} = \Delta\alpha_{l-(q,g)}\Delta T\,, \tag{1}$$

where $\Delta\alpha$ is the difference between the volume coefficient of thermal expansion of the Vit1 liquid $\alpha_l = 53\cdot10^{-6}\ K^{-1}$ [18] and the volume coefficient of thermal expansion of the solid container, which could either primarily be fused silica SiO_2 $\alpha_q = 1.5\cdot10^{-6}\ K^{-1}$ or glassy Vit1 $\alpha_g = 34\cdot10^{-6}\ K^{-1}$ [18]. Fused silica has a remarkably low α, if SiO_2 is the main container, it will act as a near constant volume container. The Vit1 shell would shrink considerably by comparison. From simple arithmetic we see that $\Delta\alpha_{l\text{-}q} \approx 51\cdot10^{-6}\ K^{-1}$ and

$\Delta\alpha_{l\text{-}g} \approx 19\cdot10^{-6}\ \mathrm{K}^{-1}$. We calculate the upper bound of negative hydrostatic pressure P_{max} in a small amount of liquid that we assume remains at the initial temperature T_o, by

$$P_{\max(q,g)} = -B_{liq}(T_o)\varepsilon_{\max} = -B_{liq}(T_o)(\alpha_l - \alpha_g)(T_o - T_g)\,. \tag{2}$$

We list these P_{max} values for both a Vit1 and SiO_2 shell in table 5.1. Figure 5.6 shows $P_{max,g}$ vs. sphere volume for all the cavitation experiments. The blue crosses represent samples that cavitated heterogeneously, the red circles represent samples that cavitated homogeneously, and the green triangles represent samples that did not cavitate at all. The smallest spheres had a tendency to avoid heterogeneous nucleation, while the larger spheres all cavitated heterogeneously, regardless of their P_{max}. To get a better understanding of how this happened we can inspect the ratio of the cavity volume to sphere volume ε_{cav}. The quantity ε_{cav} is the value of strain that is actually realized in the experiment by the cavity, so we can compare this realized strain ε_{cav} to ε_{max} for a Vit1 and SiO_2 shell. We express this quantity as a percentage in table 5.1; a quick look shows that the volume strain of the heterogeneously nucleated cavities ε_{cav} is generally 1%. This can also be seen in figure 5.7, where the sphere volume is plotted against the ratio of cavity volume to sphere volume. The 1% strain is almost 2 times larger than the maximum strain predicted from having a Vit1 shell, but only a little over half the strain predicted from a SiO_2 shell. Thus, it is impossible for a Vit1 glassy shell to have provided the containment of the liquid. Apparently, the liquid in the neck solidified too quickly for a glassy Vit1 shell to uniformly coat the inside the fused silica ampule. We see in both figure 5.6 and 5.7 that all of the heterogeneous cavitation occurred in the spheres with volumes larger than ~1 cm^3. It appears that as soon as the liquid in the neck solidified, the liquid supported only a small

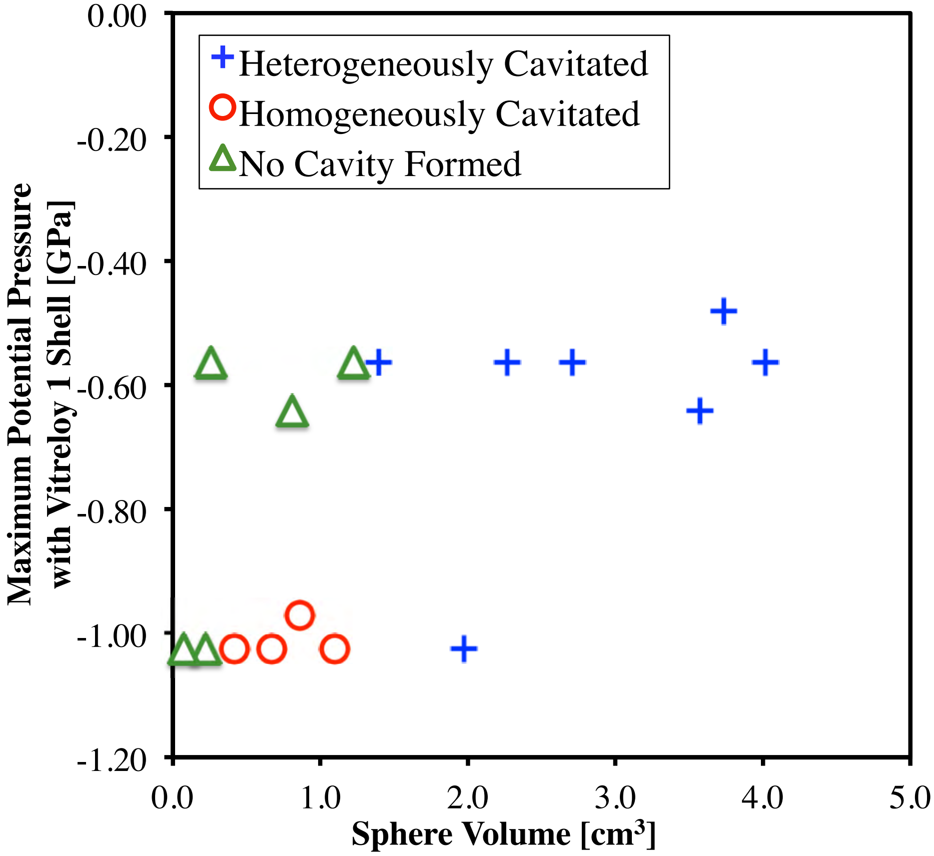

Figure 5.6 The maximum potential negative pressure that could be generated inside a sphere of liquid Vit1 if it was encapsulated inside an infinitely rigid container of glassy Vit1 and quenched quasistatically. This maximum negative pressure is estimated by $P_{\max,g} = -B_{liq}(T_o)(\alpha_l - \alpha_g)(T_o - T_g)$, where $B_{liq}(T_o)$ is the bulk modulus of the liquid at the initial temperature T_o, T_g is the glass transition temperature, α_l is the volume coefficient of thermal expansion of the liquid, and α_g is the volume coefficient of thermal expansion of the glass.

amount of negative pressure before a cavity would nucleate heterogeneously from the fused silica wall. From this point on, the fused silica sphere essentially acts as a rigid container during the remaining cooling of the liquid. The barrier to heterogeneous nucleation is lower than the barrier to homogeneous nucleation, and the rate of nucleation is higher for liquids at high temperatures, thus yielding cavities that form early and grow to be very large and highly elongated. This heterogeneous nucleation process is an important factor when considering metallic glasses as real world engineering materials. It is often possible for inclusions, amorphous or crystalline, to make their way in to the melt of a metallic glass and then be trapped in the glass during vitrification. If this same glass is then plastically deformed and has shear bands developing in the material, these inhomogeneities could act as heterogeneous nucleation sites for the formation of cavities inside the shear bands. This cavitation creates voids in the shear band that could then gather and open the shear band in to a crack, which limits the resistance to fracture of the material. Therefore, the careful control of impurities and inclusions in metallic glass will likely play a crucial role in ensuring the safety and reliability of metallic glass when it is used in an application where catastrophic failure must be avoided.

For spheres with volume strains of ~1% and lower, we observed zero heterogeneously nucleated cavities. A protective glassy shell of Vit1 must have covered the inside of the fused silica ampule before any significant negative pressure was generated in the liquid. This means that we lost some portion of our some thermal volume strain potential before the liquid was mechanically encapsulated. However, we still witnessed homogeneously nucleated cavities that were centrally located with uniform diameter cavities in four different experiments. The location and shape of these cavities leads us to believe that they nucleated homogeneously from the liquid after a critical pressure and waiting time was reached in the liquid. This cavitation rate is highly pressure- and temperature-dependent [11], but we unfortunately do not know what the exact temperature or pressure was when our Vit1 liquid cavitated. However, we do know that it nucleated homogeneously in a sample size of ~0.5 cm^3 to ~1 cm^3 on the order of 7 s. If we look at figure 5.6, we see that spheres below 0.4 cm^3 in volume with a P_{max} of 1 GPa did not cavitate at all. We also see that spheres of any volume with a P_{max} of ~0.6 GPa either did not cavitate or cavitated heterogeneously, which has a lower critical pressure than homogeneous cavitation. In particular, if you inspect the 0.75 cm^3 spheres of figure 5.5, they are of similar diameter but the one quenched from 1000 ºC cavitated homogeneously and the sphere quenched from 700 ºC did not. The sphere quenched from 700 ºC had to have some amount of negative pressure trapped in its frozen state as the entirety of its –0.6 GPa P_{max} could not have dissipated before the liquid was fully encapsulated. In addition, if we look back to figure 5.6 and inspect slightly larger spheres of ~1 cm^3 with a P_{max} of ~0.6 GPa (T_o ~650 ºC), there is a transition from no cavity to heterogeneous nucleation for two spheres that are similar in volume. Again, the sphere without a cavity must have supported some amount of negative pressure that contributed to the heterogeneous cavitation of the similarly sized sphere. Thus, we have established that the Vit1 liquid is "metastable" on laboratory timescales, temperatures, and negative pressures. At some critical negative pressure the liquid will decompose in to a Vit1 liquid and a cavity, but at some negative pressure that does not reach a critical value, the Vit1 liquid remains a single phase and solidifies into a cavity-free glass.

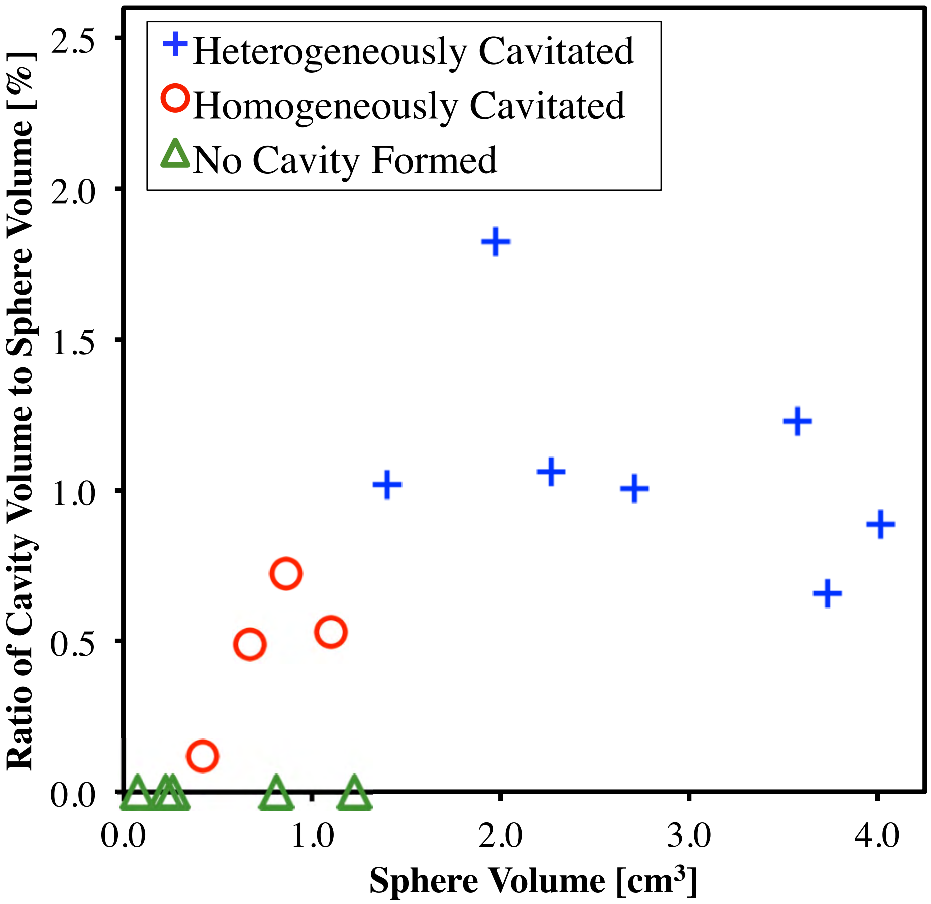

Figure 5.7 Cavity volume as a percentage of the sphere volume versus the sphere volume. Spheres with volumes much larger than 1 cm^3 always heterogeneously nucleated cavities from the wall of the fused silica container. These large volume spheres were unable to form a protective shell of glassy Vit1 on the inside of the fused silica container before significant negative pressure was generated in the liquid. The smaller diameter spheres with homogeneously nucleated cavities were able to grow a protective shell of glassy Vit1 before negative pressure was generated. This enabled the liquid to support a much greater amount of negative pressure upon subsequent cooling, as the barrier for homogeneous nucleation is higher than for heterogeneous nucleation.

To inspect the actual pressures more closely, we can use ε_{cav} to estimate the negative pressure P_{cav} that was present in the sphere at the point the cavity began to grow. We multiply this strain by the bulk modulus of appropriate temperature and estimate this strain as a negative pressure, listed in table 5.1 and overlaid on figure 5.8, the plot of ε_{cav} versus sphere volume. Note that we focus figure 5.8 on the experimental range that did not produce any heterogeneously nucleated cavities. The blue squares, red circle, purple diamond, and green triangles are the spheres quenched from 1000 ºC, 950 ºC, 700 ºC, and 650 ºC, respectively. Since none of these spheres cavitated heterogeneously, they were likely encapsulated in a glassy shell of Vit1. Because of this, the maximum negative pressure should be estimated with the assumption of a solid Vit1 shell, instead of a solid fused silica shell. The Vit1 solid shell P_{max} is shown in the legend of figure 5.8 for each T_o, it descends from –1.02 GPa to –0.56 GPa. All of the samples quenched from 700 ºC and below did not cavitate. All of the samples quenched from 950 ºC and above cavitated as long as the sphere volume was greater than 0.4 cm^3. The average P_{cav} for spheres that were larger than 0.5 cm^3 was roughly –500 MPa. A notable exception is the one sphere that was quenched from 1000 ºC with a P_{cav} of only –100 MPa. This sphere was the smallest sphere to cavitate at a volume of 0.42 cm^3. Since it had the same nominal starting temperature (same cavitation rate and critical pressure associated with that temperature) as its larger siblings, it is a curiosity that its cavity grew to be one fifth of their cavity sizes. This is probably due to the dynamic nature of the quenching in this experiment and represents a size, critical pressure, or time cutoff necessary for the nucleation and growth of a cavity. It is also possible that all of the cavities nucleated homogeneously at –100 MPa and then continued to grow because the larger spheres had extra thermal volume strain to continue cavity growth. If this is true it informs us that a sphere of 0.5 cm^3 to 1 cm^3 loses approximately –500 MPa of its equivalent thermal volume strain before the liquid is fully encapsulated. Thus, a 0.5 cm^3 to 1 cm^3 volume sphere with a P_{max} of –600 MPa might barely cross the critical negative pressure threshold of –100 MPa or it might solidify with the negative pressure as a residual stress. A detailed finite element model that included all the fine details of this experiment would be of great use in analyzing the negative pressures, temperatures, and timescales necessary to homogeneously nucleate cavities in the $Zr_{41.2}Cu_{12.5}Ti_{13.8}Be_{22.5}Ni_{10}$ liquid.

Table 5.1 Results summary for the cavitation experiments on the $Zr_{41.2}Cu_{12.5}Ti_{13.8}Be_{22.5}Ni_{10}$ (Vit1) liquid. The sphere volume, initial temperature T_o, ΔT (difference between T_o and T_g), estimated thermal volume strain for a Vit1 or fused silica shell, temperature-dependent bulk modulus of Vit1 B(T_o) [17], maximum potential negative pressure for a sphere with a Vit1 or fused silica shell, cavity nucleation type, cavity volume as the ratio of sphere volume, cavity strain as a percentage of the maximum thermal strain for a Vit1 or fused silica shell, and the negative pressure estimated from the volume strain of the cavity for every cavitation experiment of the Vit1 liquid.

Sphere Diameter [mm]	Sphere Volume [cm^3]	Initial Temperature (T_o) [°C]	ΔT (T_o-T_g) [°C]	Maximum Potential Volume Strain $\Delta T \cdot \Delta\alpha_{l\text{-}g}$ (Vit1 shell) [–]	Maximum Potential Volume Strain $\Delta T \cdot \Delta\alpha_{l\text{-}q}$ (SiO_2 shell) [–]	Vit1 Bulk Modulus at T_o, B(T_o) [GPa]	Maximum Potential Pressure with a Vit1 Shell [GPa]	Maximum Potential Pressure with a Fused Silica Shell [GPa]	Cavity Nucleation Type	Cavity Volume as Ratio of Sphere Volume [%]	Potential Strain Realized in Cavity with Vit1 Shell [%]	Potential Strain Realized in Cavity with Fused Silica Shell [%]	Pressure from Cavity Volume Strain Ratio (P_{cav}) [GPa]
19.3	3.74	600	255	0.005	0.013	99.2	-0.48	-1.30	Heterogeneous	0.66	139	51	0.67
13.9	1.40	650	305	0.006	0.016	97.1	-0.56	-1.53	Heterogeneous	1.02	178	66	1.00
16.3	2.27	650	305	0.006	0.016	97.1	-0.56	-1.53	Heterogeneous	1.06	186	69	1.05
17.3	2.71	650	305	0.006	0.016	97.1	-0.56	-1.53	Heterogeneous	1.01	177	65	1.00
19.7	4.02	650	305	0.006	0.016	97.1	-0.56	-1.53	Heterogeneous	0.89	156	58	0.88
19.0	3.57	700	355	0.007	0.018	95.0	-0.64	-1.74	Heterogeneous	1.23	185	68	1.19
15.6	1.97	1000	655	0.012	0.034	82.4	-1.02	-2.78	Heterogeneous	1.82	145	53	1.49
11.6	0.81	700	355	0.007	0.018	95.0	-0.64	-1.74	None	0	0	0	0
7.9	0.26	650	305	0.006	0.016	97.1	-0.56	-1.53	None	0	0	0	0
13.3	1.23	650	305	0.006	0.016	97.1	-0.56	-1.53	None	0	0	0	0
7.5	0.22	1000	655	0.012	0.034	82.4	-1.02	-2.78	None	0	0	0	0
5.2	0.07	1000	655	0.012	0.034	82.4	-1.02	-2.78	None	0	0	0	0
10.9	0.67	1000	655	0.012	0.034	82.4	-1.02	-2.78	Homogeneous	0.49	41	15	0.42
12.8	1.10	1000	655	0.012	0.034	82.4	-1.02	-2.78	Homogeneous	0.53	43	16	0.44
9.3	0.42	1000	655	0.012	0.034	82.4	-1.02	-2.78	Homogeneous	0.12	10	4	0.10
11.8	0.86	950	605	0.011	0.031	84.5	-0.97	-2.63	Homogeneous	0.72	63	23	0.62

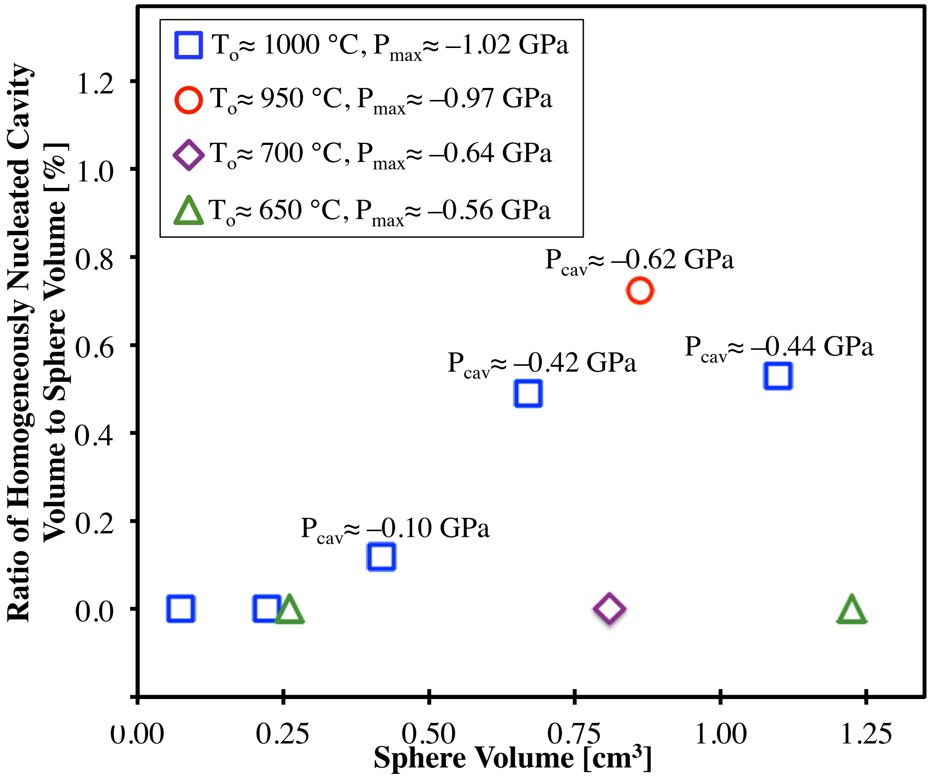

Figure 5.8 The volume strain of the homogeneously nucleated cavities vs. the sphere volume. The blue squares, red circle, purple diamond, and green triangles are the spheres quenched from T_o = 1000 ºC, 950 ºC, 700 ºC, and 650 ºC, respectively. The maximum negative pressure P_{max} that can be achieved inside an infinitely rigid shell of Vit1 glass is shown in the legend for each T_o. For the spheres that did cavitate, the pressure in the sphere at the point of cavitation P_{cav} is estimated from the volume strain of the cavity ε_{cav} and is displayed next to the markers. No sphere quenched from ~700 ºC or with a volume smaller than 0.4 cm^3 formed cavities. The spheres that did homogeneously cavitate had –100 to –600 MPa of available thermal volume strain in the sphere. The smallest value, –100 MPa may represent the critical cavitation pressure of the Vit1 liquid at 1000 ºC on the laboratory timescale of 1 to 7 s.

Preliminary results from the Vit1 experiments were used by An, Garrett, et al. [11] to provide a real, even if tenuous, experimental underpinning to the determination of the MD cavitation rate in a CuZr liquid. The MD simulations showed that cavitation in the liquid is a stochastic waiting process characterized by Poisson statistics. The 54,000 atom system cavitated with a mean waiting time of 97 ps for a pressure of –3.16 GPa and temperature of 1200 K. The waiting time was then determined at three different pressures also at 1200 K. When the waiting time vs. negative pressure was fit quadratically, we found that at laboratory timescale of 7 s and system size of 10^{22} atoms we extrapolated that would occur at –500 MPa. This is a very reasonable prediction that is supported by the current experimental results, especially given the 27 orders of magnitude covered by the extrapolation.

In conclusion, we used the experimental data combined with simple analytic modeling to estimate the critical pressure for cavitation as a function of temperature in liquid Vit1. We estimate that centimeter diameter spheres of Vit1 at ~1000 ºC homogeneously cavitate with less than –500 MPa of pressure at laboratory timescales of 1 to 7 s. We also find that cavitation does not occur in a ~700ºC Vit1 liquid with a laboratory timescale of 1 to 7 s and some fraction of the –500 MPa pressure that caused cavitation in the ~1000 ºC liquid. The Vit1 liquid is thus “metastable” on laboratory timescales with respect to cavitation at these temperatures and estimated negative pressures. Heterogeneous nucleation was promoted whenever liquid Vit1 is subjected to negative pressures while in contact with fused silica, an important consideration as this shortcut to cavitation could severely limit the damage tolerance of metallic glasses.

BIBLIOGRAPHY

[1] M. D. Demetriou, M. E. Launey, G. Garrett, J. P. Schramm, D. C. Hofmann, W. L. Johnson, and R. O. Ritchie, Nat Mater **10**, 123 (2011).

[2] M. E. Launey, D. C. Hofmann, J. Y. Suh, H. Kozachkov, W. L. Johnson, and R. O. Ritchie, Appl Phys Lett **94**, 241910 (2009).

[3] R. O. Ritchie, Nat Mater **10**, 817 (2011).

[4] J. J. Lewandowski, W. H. Wang, and A. L. Greer, Philosophical Magazine Letters **85**, 77 (2005).

[5] E. Bouchaud, D. Boivin, J. L. Pouchou, D. Bonamy, B. Poon, and G. Ravichandran, Epl-Europhys Lett **83**, (2008).

[6] J. Suh, R. Conner, C. Kim, and M. Demetriou, in *Proceedings of the SEM Annual Conference* (2009).

[7] J. J. Lewandowski and A. L. Greer, Nat Mater **5**, 15 (2005).

[8] W. L. Johnson, M. D. Demetriou, J. S. Harmon, M. L. Lind, and K. Samwer, Mrs Bull **32**, 644 (2007).

[9] C. E. Brennen, *Cavitation and Bubble Dynamics* (Oxford University Press, New York, 1995).

[10] G. Duan, Simulations, Modeling, and Designs of Bulk Metallic Glasses, California Institute of Technology, 2008.

[11] Q. An, G. Garrett, K. Samwer, Y. Liu, S. V. Zybin, S.-N. Luo, M. D. Demetriou, W. L. Johnson, and W. A. Goddard, J Phys Chem Lett **2**, 1320 (2012).

[12] P. Murali, T. Guo, Y. Zhang, R. Narasimhan, Y. Li, and H. Gao, Phys Rev Lett **107**, (2011).

[13] M. L. Lind, Ultrasonic Investigation of the Elastic Properties and Liquid Fragility of Bulk Metallic Glasses in the Supercooled Liquid Region, California Institute of Technology, 2008.

[14] M. Bertholet, Ann. Chim. Phys. **30**, 232 (1850).

[15] A. R. Imre, AIP Conf. Proc. **1349**, 33 (2011).

[16] W. Johnson and K. Samwer, Phys Rev Lett **95**, 195501 (2005).

[17] M. L. Lind, G. Duan, and W. L. Johnson, Phys Rev Lett **97**, 015501 (2006).

[18] K. Ohsaka, S. K. Chung, W. K. Rhim, A. Peker, D. Scruggs, and W. L. Johnson, Appl Phys Lett **70**, 726 (1997).